JOC The Journal of Organic Chemistry

Article

pubs.acs.org/joc

Donor-Substituted Octacyano[4]dendralenes: Investigation of π-Electron Delocalization in Their Radical Ions

Benjamin Breiten,[†] Markus Jordan,[†] Daisuke Taura,[†] Michal Zalibera,[‡] Markus Griesser,[‡] Daria Confortin,[‡] Corinne Boudon,[§] Jean-Paul Gisselbrecht,[§] W. Bernd Schweizer,[†] Georg Gescheidt,*[,‡] and François Diederich*[,†]

[†]Laboratory of Organic Chemistry, ETH Zurich, Hönggerberg, HCI, CH-8093 Zurich, Switzerland

[‡]Institute of Physical and Theoretical Chemistry, Graz University of Technology, Stremayrgasse 9, A-8010 Graz, Austria

[§]Laboratoire d'Electrochimie et de Chimie Physique du Corps Solide, UMR 7177 CNRS, Université de Strasbourg, 4 rue Blaise Pascal, F-67081 Strasbourg Cedex, France

Supporting Information

ABSTRACT: Symmetrically and unsymmetrically electron-donor-substituted octacyano[4]dendralenes were synthesized and their opto-electronic properties investigated by UV/vis spectroscopy, electrochemical measurements (cyclic voltammetry (CV) and rotating disk voltammetry (RDV)), and electron paramagnetic resonance (EPR) spectroscopy. These nonplanar push–pull chromophores are potent electron acceptors, featuring potentials for first reversible electron uptake around at −0.1 V (vs Fc^+/Fc, in CH_2Cl_2 + 0.1 M n-Bu_4NPF_6) and, in one case, a remarkably small HOMO–LUMO gap (ΔE = 0.68 V). EPR measurements gave well-resolved spectra after one-electron reduction of the octacyano[4]dendralenes, whereas the one-electron oxidized species could not be detected in all cases. Investigations of the radical anions of related donor-substituted 1,1,4,4-tetracyanobuta-1,3-diene derivatives revealed electron localization at one 1,1-dicyanovinyl (DCV) moiety, in contrast to predictions by density functional theory (DFT) calculations. The particular factors leading to the charge distribution in the electron-accepting domains of the tetracyano and octacyano chromophores are discussed.

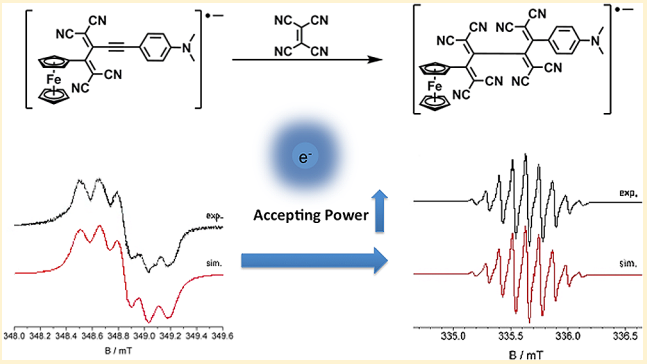

1. INTRODUCTION

π-Conjugated donor–acceptor (D–A) chromophores[1] have recently attracted renewed interest in view of potential applications in the fabrication of opto-electronic materials.[2] The energy and intensity of their characteristic intramolecular charge-transfer (CT) transitions as well as their third-order optical nonlinearities depend both on the strength of the electron donor and acceptor moieties and the nature of the connecting π-conjugated spacer.[3] Numerous potent organic electron acceptors are cyano-rich derivatives, taking advantage of the strong electron-accepting power of the cyano group, as compared to its low molecular weight.[4] Tetracyanoethene (TCNE)[5] and 7,7,8,8-tetracyano-*p*-quinodimethane (TCNQ),[6] together with their derivatives and analogues,[7] are possibly the most prominent and most widely used representatives.

TCNE readily reacts with organo-donor-activated CC triple bonds to provide, via a formal [2 + 2] cycloaddition followed by retro-electrocyclization, donor-substituted 1,1,4,4-tetracyanobuta-1,3-dienes.[8] The scope of this versatile transformation is very broad.[9] The nature of both the donor, which activates the alkyne, and the electron-deficient olefin can be greatly varied, yielding entire new families of nonplanar push–pull chromophores.[2e,f,10] Recently, we reported the first double addition of TCNE to the two adjacent CC triple bonds in symmetric, 1,4-dianilino-substituted buta-1,3-diynes under formation of donor-substituted octacyano[4]dendralenes.[11] These novel chromophores, despite their pronounced nonplanarity, feature strong intramolecular CT interactions as well as a high propensity for reversible electron uptake. Initial electron paramagnetic resonance (EPR) measurements provided evidence for the formation of charge-separated paramagnetic species pointing to delocalized organic radical anions in which the spin population mainly resides at cyano group-containing moieties.

Here, we report a comprehensive study of the opto-electronic properties of symmetrically and unsymmetrically donor-substituted octacyano[4]dendralenes **1**–**3** and compare these properties to those of related 1,1,4,4-tetracyanobuta-1,3-dienes (TCBDs) **4** and **5**. The report has a special focus on the radical ions of these systems that are investigated in a combined experimental (EPR) and computational approach.

Special Issue: Howard Zimmerman Memorial Issue

Received: June 12, 2012
Published: July 10, 2012

Scheme 1. Syntheses of Octacyano[4]dendralenes 1−3

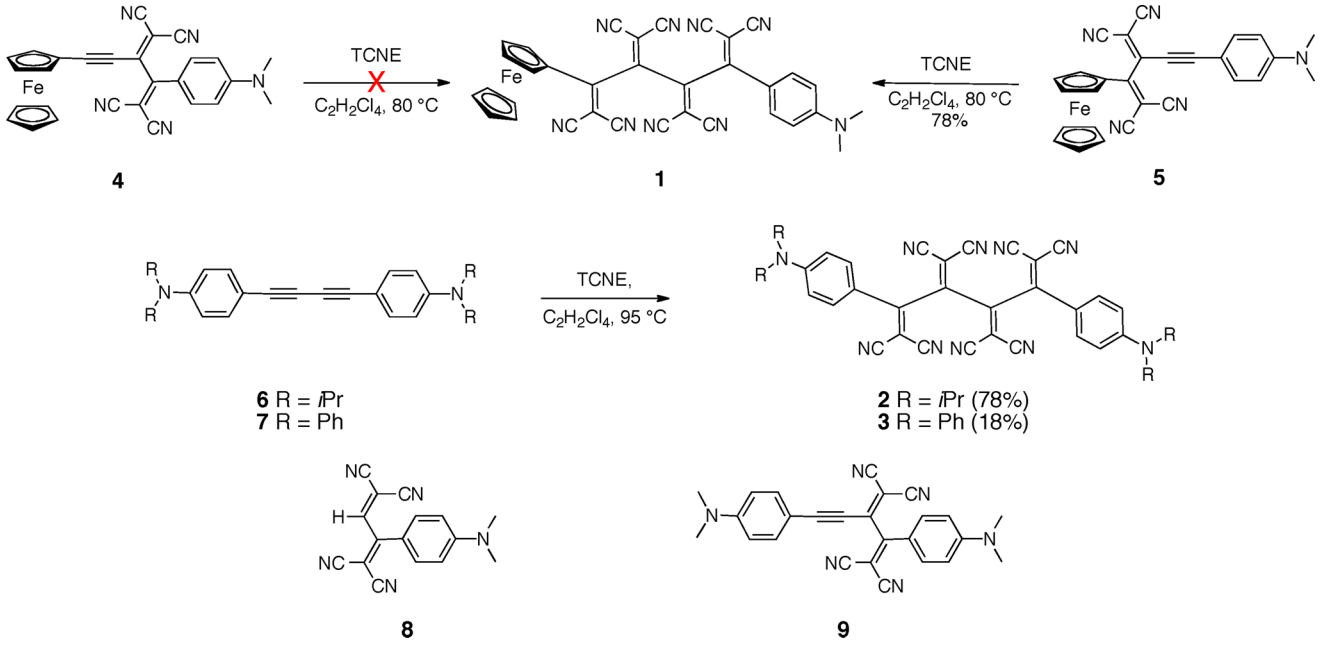

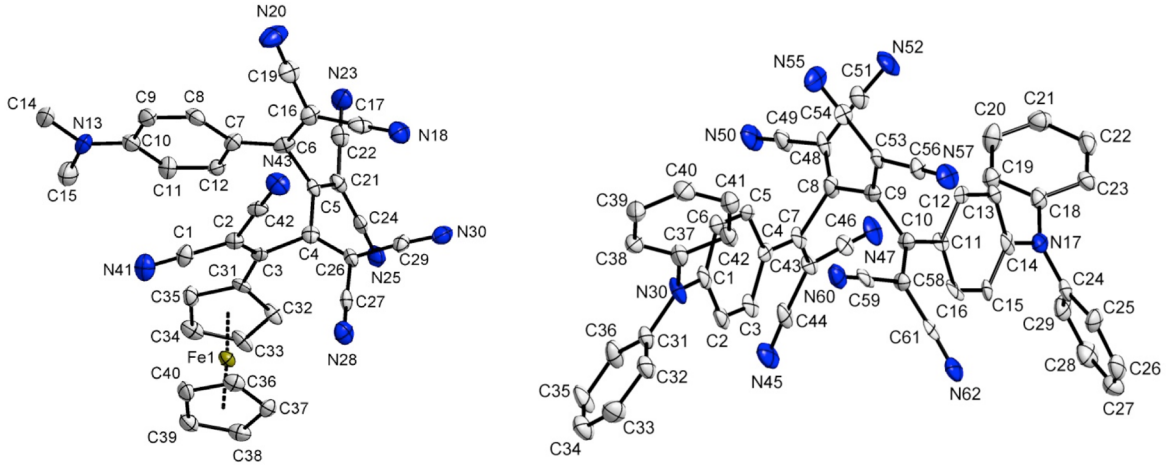

Figure 1. ORTEP plots of the solid-state molecular structures of **1** (left) and **3** (right). T = 100 K. Thermal ellipsoids are drawn at the 50% probability level; arbitrary numbering; hydrogen atoms are omitted for clarity. Selected dihedral angles in **1** [°]: C3−C4−C5−C6 56.2(5), C21−C5−C6−C16 −91.6(5), C2−C3−C4−C26 88.3(6), C26−C4−C5−C21 60.4(6). Selected dihedral angles in **2** [°]: C7−C8−C9−C10 50.1(7), C43−C7−C8−C48 68.5(9), C48−C8−C9−C53 56.0(9), C53−C9−C10−C58 66.2(8).

2. RESULTS AND DISCUSSION

2.1. Synthesis. Recently, we found that the regioselectivity of the TCNE addition to a buta-1,3-diyne end-capped with a ferrocenyl (Fc) and a *N*,*N*-dimethylanilino (DMA) donor can be switched upon changing the pH.[12] At neutral pH, DMA is the better activator (Hammett constants σ_p^+: Fc, − 1.00; NMe_2, −1.70),[13] and cycloaddition/retro-electrocyclization (CA/RE) occurs at the adjacent triple bond, yielding TCBD **4** (98% yield). Upon protonation of the anilino group, activation by Fc dominates and leads, after neutralization, to the formation of the regioisomeric TCBD **5** (83%). Interestingly, monoadduct **4** did not undergo a second CA/RE reaction to the desired bis-adduct **1**, even with an excess of TCNE at 80 °C and at prolonged reaction time. On the other hand, the stronger electron donor DMA in monoadduct **5** enabled the second cycloaddition, and the unsymmetrically donor-substituted octacyano[4]dendralene **1** was obtained in good yield (78%; Scheme 1). For comparison, in the physical studies, we also prepared by a one-pot protocol the octacyano[4]dendralenes **2**[11] and **3**, starting from buta-1,3-diynes **6** and **7**, respectively. The known TCBDs **8** and **9** served as additional control compounds.[8b]

For octacyano[4]dendralenes **1** and **3**, NMR spectra could not be recorded due to the presence of paramagnetic species in the sample, as confirmed by electron paramagnetic resonance (EPR) spectroscopy. Therefore, we turned to X-ray crystallography in order to establish their structures in an unambiguous way.

2.2. X-ray Structures of Octacyano[4]dendralenes 1 and 3. Crystals suitable for X-ray diffraction were obtained by layering solutions of **1** or **3** in CH_2Cl_2 with *n*-hexane and subsequent slow evaporation of the solvents. Dendralene **1** crystallizes in the monoclinic space group $P2_1/c$. The molecular structure (Figure 1 left) shows a *syn*-conformation of the donor

dx.doi.org/10.1021/jo301194y | J. Org. Chem. 2013, 78, 1760−1767

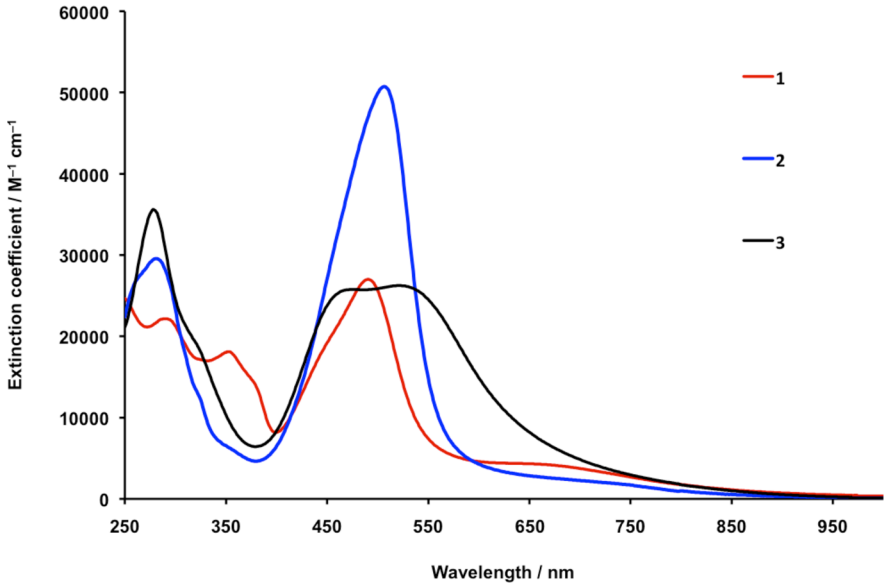

Figure 2. UV/vis absorption spectra of **1**–**3** in CH_2Cl_2 at 298 K ($c \sim 10^{-5}$ M).

substituents in the solid state, with a torsion angle of the dendralene backbone (C3–C4–C5–C6) of 56.2(5)°. A similar *syn*-conformation had previously been observed for the solid-state structure of octacyano[4]dendralene **2**.[11] In this geometry, all eight cyano groups converge into one hemisphere, whereas the Fc and the DMA donor moieties point into the other. The angles between the donor planes (phenyl ring of DMA and substituted Cp ring of Fc) and their adjacent dicyanovinyl (DCV) acceptor groups are almost matching (23.1° and 23.2°) and close to planarity, allowing efficient intramolecular CT interactions. However, two of the three dihedral angles between the four DCV substituents on the dendralene backbone are close to perpendicularity (between 86.0(5)° and 95.0(5)°; see Figure 1 left), leading to particular electronic effects (see below). This sterical arrangement induces a certain helicity of the dendralene backbone as well as a favorable dipolar interaction between the nitrile group C42≡N43 of the DCV next to the Fc substituent and the DCV moiety C6═C16$(CN)_2$ adjacent to the anilino donor (d(N43···C6) = 3.42 Å). This interaction might actually be a reason for the *syn*-alignment of the donor substituents.

Compound **3** crystallizes in the triclinic space group $P\bar{1}$ with two CH_2Cl_2 molecules in the asymmetric unit. The solid-state geometry of **3** (Figure 1 right), with bulky terminal triarylamine donor moieties, differs substantially from the one of compound **1**. Although the torsion angle (C7–C8–C9–C10) of the central dendralene fragment of **3** is quite similar in **3** (50.1(7)°) and in **1** (56.2(5)°), the molecule adopts an extended *anti*-conformation, probably because of steric repulsion between the two triarylamino groups in a *syn*-arrangement. The bulkiness of these groups forces a denser arrangement of the DCV moieties on the [4]dendralene scaffold of **3**, with substantially smaller dihedral angles between 50.1(7)° and 68.1(9)° as compared to **1**. Furthermore, the angles between the aniline donors and the second neighboring DCV moiety in **3** (C4–C7–C8–C48 −116.2(7)°; C53–C9–C10–C11 −115.7(6)°) are significantly more obtuse than the corresponding angles in **1** (C31–C3–C4–C26 −95.0(5)°; C21–C5–C6–C7 90.8(6)°). The angles between the planes of the anilino moieties and their directly adjacent DCV groups (30.3° and 22.3°) are, however, similar to the corresponding angles in **1**.

2.3. Electronic Absorption Spectra. The UV/vis spectra of chromophores **1**–**3** display two bathochromically shifted intramolecular CT bands with absorptions reaching into the near-infrared (NIR) region (Figure 2). Support for the CT character of these bands was obtained by protonation with CF_3COOH, which led to their disappearance for compound **2** and **3**, while subsequent reneutralization restituted the absorption bands, as previously described.[14] Protonation of a solution of **1** with CF_3COOH shows only a reduction of the CT band, while subsequent reneutralization restituted the absorption bands. A complete disappearance of the CT band could not be observed due to the presence of the ferrocene donor, which is not protonated. The intense CT band at higher energy (λ_{max} around 500 nm) involves the transition from the donors to the adjacent, nearly coplanar and hence strongly π-coupled DCV acceptor.[15] The low-intensity, low-energy CT transition at around 700 nm involves weakly π-coupled donor and acceptor moieties and most probably results from CT from an anilino to the cross-conjugated TCBD moiety at the center of the molecules.

2.4. Electrochemistry. The electron-transfer properties of **1**, **2**,[11] and **3** were investigated by cyclic (CV) and rotating disk voltammetry (RDV), and the corresponding potentials are summarized in Table 1. For some derivatives, reproducible data could only be observed on freshly polished working electrodes due to electrode inhibition during redox processes.

The anilino donor in octacyano[4]dendralene **1** is responsible for the one-electron irreversible oxidation at +1.07 V, compatible with related potentials of DMA oxidation in TCBD derivatives.[8b] However, the oxidation potential is 320 mV anodically shifted compared to that of the anilino moiety in TCBD **4**.[12] The influence of the octacyano[4]dendralene acceptor on the oxidation potential of the Fc moiety is less pronounced, with a reversible one-electron oxidation at +0.57 V (**5**: +0.49 V).[12] The voltammogram of [4]dendralene **3** can be interpreted in terms of an irreversible two-electron oxidation connected with the precipitation of the oxidized species at the electrode surface. Indeed, in the reverse scan, a reduction peak

dx.doi.org/10.1021/jo301194y | J. Org. Chem. 2013, 78, 1760–1767

Table 1. Cyclic Voltammetry (CV; Scan Rate v = 0.1 V s^{-1}) and Rotating Disk Voltammetry (RDV); Solvent CH_2Cl_2 (+0.1 M n-Bu_4NPF_6)[a]

	CV			RDV	
compd	E^{o}[b] (V)	ΔE_p[c] (mV)	E_p[d] (V)	$E_{1/2}$[e] (V)	slope[f] (mV)
1			+1.07	[g]	
	+0.57 (1e$^-$)	80		+0.56 (1e$^-$)	60
	−0.11 (1e$^-$)	80		−0.12 (1e$^-$)	60
	−0.63 (1e$^-$)	100		−0.64 (1e$^-$)	90
	−1.60 (1e$^-$)	70		−1.59 (1e$^-$)	60
	−1.78 (1e$^-$)	60		−1.76 (1e$^-$)	110
2[h]	+0.99 (2e$^-$)	70		+0.98 (2e$^-$)	60
	−0.08 (1e$^-$)	70		−0.09 (1e$^-$)	75
	−0.58 (0.5e$^-$)	60		−0.62 (1e$^-$)	85
	−0.66 (0.5e$^-$)	60		−1.70 (2e$^-$)	140
	−1.56 (1e$^-$)	70			
	−1.71 (1e$^-$)	70			
3			+0.93	+0.89 (2e$^-$)	60
	−0.08 (1e$^-$)	75		−0.08 (1e$^-$)	60
	−0.57 (1e$^-$)	90		−0.60 (1e$^-$)	70
	−1.47 (1e$^-$)	80		−1.50 (1e$^-$)	70
	−1.68 (1e$^-$)	80		−1.71 (1e$^-$)	70

[a]All potentials are given versus the Fc^+/Fc couple used as the internal standard. [b]E^{o} = (E_{pc} + E_{pa})/2, where E_{pc} and E_{pa} correspond to the cathodic and anodic peak potentials, respectively. [c]ΔE_p = E_{pa} − E_{pc}. [d]E_p = irreversible peak potential. [e]$E_{1/2}$ = half-wave potential. [f]Logarithmic analysis of the wave obtained by plotting E versus $\log[I/(I_{lim} - I)]$. [g]Very small amplitude signal due to electrode inhibition. [h]Taken from ref 11.

whose shape is in agreement with redissolution is observed at +0.54 V. On the other hand, the four DCV moieties of **1** and **3** gave rise to four reversible one-electron reduction steps. The first two reductions are strongly facilitated compared with TCBD derivatives (−0.11 and −0.63 V for **1** and −0.08 and −0.57 V for **3**), revealing the lowest electrochemical HOMO−LUMO gap (ΔE = 0.68 V for **1**) ever observed for this type of D−A chromophores.[2e,f] Therefore, an efficient CT can be considered, leading to a stabilized charge-separated state.

2.5. Radical Ions of CT Chromophores 1−5. The electrochemical measurements on **1**−**5** indicated that one-electron reduction is reversible with the tetra- and octacyano moieties being the electroactive parts, whereas the corresponding oxidations present also nonreversible features. In the latter case, the first oxidation proceeds at the ferrocene moiety (**1**, **4**, **5**) in a reversible fashion. When only the anilino substituent is present (**2**, **3**), the redox potentials are in line with amine oxidation. For the triphenylamino derivative **3**, oxidation is irreversible, presumably owing to dimerization, also in line with the observed precipitations (see above). Only in the case of **2**, reversible cyclovoltammetric curves were recorded. For EPR investigations, radical ions can be formed either by chemical reactions or by electrolysis.[16] Both approaches were followed to generate radical cations of **1**−**5**; the compounds were dissolved in CH_2Cl_2 and chemically oxidized with either phenyliodine-(III) bistrifluoroacetate (PIFA) or $NOSbF_6$; moreover, anodic oxidation was performed on a Pt electrode. Although the strict high-vacuum conditions utilized for the production of the oxidized species often allow even the detection of paramagnetic species connected with irreversible cyclovoltammograms, none of the investigated molecules gave rise to clearly distinguishable EPR spectra after oxidation. In the case of **1**, **4**, and **5**, an Fe(III) species is expected. It is well established that oxidized ferrocenes give rise to EPR spectra only in the solid state at temperatures close to 4 K with characteristic signals pointing to the axial symmetry of the paramagnetic center ($g_{\|}$ = 4.3−2.6 and $g_{\perp}$ = 1.9−1.2, depending on the substitution and character of the solid matrix).[17] Therefore, it is not unexpected that we were unable to observe the corresponding signals neither in fluid nor in frozen (77 K) solution. Nevertheless, this underpins that the ferrocene unit is the electroactive part of **1**, **4**, and **5** in the oxidative regime. In the case of **3**, we were not able to detect an EPR spectrum upon chemical or electrochemical oxidation mirroring the irreversible oxidation wave in the cyclovoltammogram. Unexpectedly, also oxidation of **2** did not lead to a discernible EPR spectrum.

In the case of one-electron reduction reactions, performed chemically (Na metal in THF, cathodic reduction, see the Experimental Section) well-resolved EPR spectra could be recorded for **1**−**5**. For TCBD derivatives **4** and **5**, EPR spectra with essentially matching patterns were obtained (Figure 3).

The dominating EPR spectral patterns consist of five lines caused by the interaction of two virtually identical ^{14}N nuclei interacting with the unpaired electron (^{14}N isotropic hyperfine coupling constants, hfcs, of 0.134 and 0.151 mT for $\mathbf{4}^{\bullet-}$ and 0.154 and 0.134 mT for $\mathbf{5}^{\bullet-}$; each for 1 N). Further splittings are caused by ^{14}N hfcs of 0.040 (1 N)/0.033 mT (1 N) and

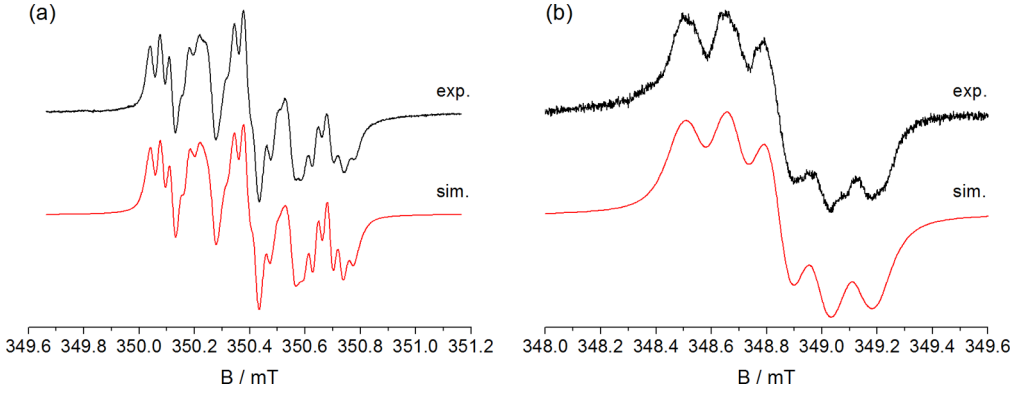

Figure 3. Experimental EPR spectra and their simulations obtained after reduction with a Na mirror in THF: (a) $\mathbf{4}^{\bullet-}$, g = 2.0035; (b) $\mathbf{5}^{\bullet-}$, g = 2.0038. Virtually identical EPR spectra were obtained upon controlled potential reduction of **4** and **5** in CH_3CN solutions (+ 0.1 M n-Bu_4NPF_6) with polarization potentials set 100 mV more negative than the $E_{1/2}$ of the first reduction step.

dx.doi.org/10.1021/jo301194y | J. Org. Chem. 2013, 78, 1760−1767

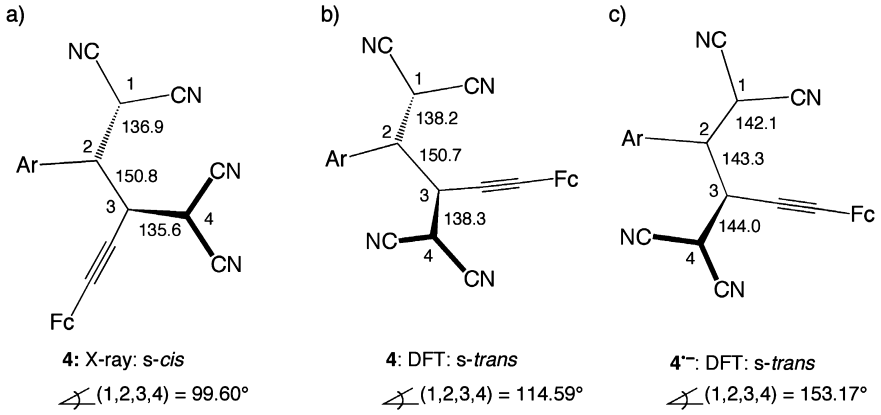

Figure 4. Geometry of the 1,1,4,4-tetracyanobuta-1,3-diene fragment: (a) parent **4** according to X-ray structure analysis. Calculated geometry (B3LYP/6-31G(d)) of (b) parent **4** and (c) of $\mathbf{4}^{\bullet-}$ (bond lengths are given in pm).

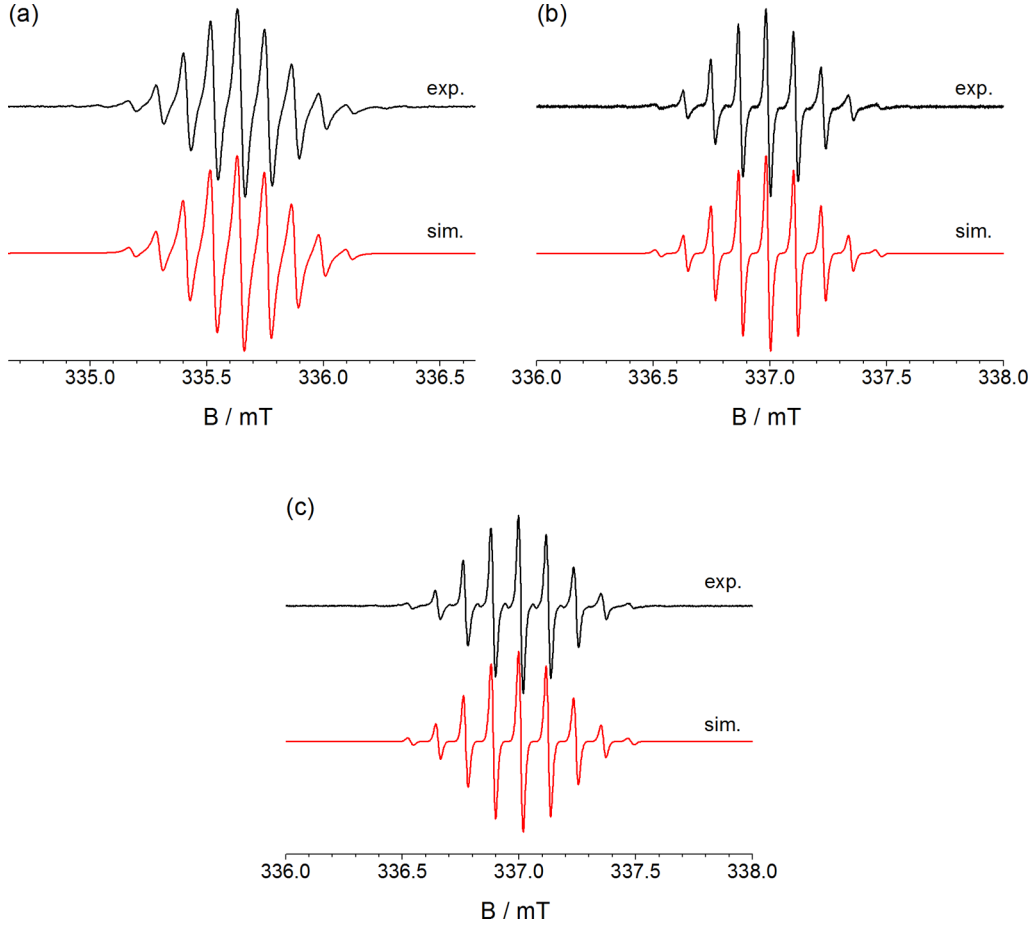

Figure 5. Experimental EPR spectra together with their simulations attributed to (a) $\mathbf{1}^{\bullet-}$, g = 2.0029, ^{14}N hfc = 0.116 mT (4 N); (b) $\mathbf{2}^{\bullet-}$ g = 2.0030, ^{14}N hfc = 0.118 mT (4 N); (c) $\mathbf{3}^{\bullet-}$, g = 2.0027, ^{14}N hfc = 0.118 mT (4 N).

0.033 mT (2 N) for $\mathbf{4}^{\bullet-}$ and $\mathbf{5}^{\bullet-}$, respectively. These data clearly reveal that the spin and the charge are not evenly distributed between the two DCV moieties. This experimental finding is rather unexpected when compared with reference acceptors **8** and **9** resembling **4** and **5** but lacking the ferrocene substituents. In $\mathbf{8}^{\bullet-}$ and $\mathbf{9}^{\bullet-}$, the DCV moieties are identical in terms of electron distribution, mirrored by the ^{14}N hfcs of 0.109 ($\mathbf{8}^{\bullet-}$) and 0.117 ($\mathbf{9}^{\bullet-}$) mT, each attributed to four virtually equivalent nitrogen nuclei.[8c] Indeed, taking the X-ray crystal structure[12] of **4** as the starting point for geometry optimization of the radical anion (B3LYP/6-31G(d)), the initial dihedral angle C1−C2−C3−C4, representing the twist around the central buta-1,3-diene bond, decreases from an s-*cis*-type arrangement (99.60°) to s-*trans* (153.17°, Figure 4).

The theoretically determined hfcs connected with this optimized geometry show almost identical values for the four cyano nitrogen atoms. This is in clear contrast with the experimental values, which show that the two DCV moieties are distinctly inequivalent. To investigate the quality of the theoretical prediction, two routes were pursued:

dx.doi.org/10.1021/jo301194y | J. Org. Chem. 2013, 78, 1760−1767

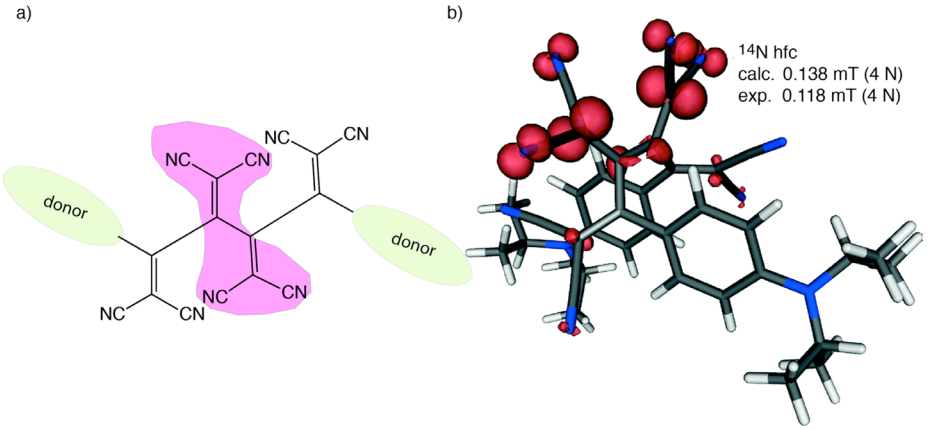

Figure 6. (a) Sketch of the spin distribution in $2^{\bullet-}$ (as representative example for $1^{\bullet-}$–$3^{\bullet-}$) and (b) the corresponding singly occupied orbital including the calculated and experimental hfcs (the calculated data are averaged from the four almost equivalent values, cf. the Supporting Information).

(i) We calculated (DFT) the geometry of **4** and compared it with the experimental X-ray data (see the Supporting Information). Remarkably, the two geometries show significant deviations: The calculation leads to an s-*trans* conformation, whereas the X-ray structure is rather close to an s-*cis* arrangement of the butadiene (Figure 4). The calculated hyperfine data for $4^{\bullet-}$ employing the X-ray structure indicate substantial delocalization of the spin into the aniline fragment causing well distinguishable ^{1}H hfcs, which, however, do not correspond to the experimental data.

(ii) We aligned the molecular arrangement of the relaxed DFT structure to that of the parent X-ray structure and calculated the hfcs in a single-point procedure. In this case, the theoretical data match rather well with the experimental counterparts.

Apparently, in the case of the strongly polarized push–pull molecules, calculations experience several superimposed complications. It has been established that in some cases DFT calculations using hybrid functionals (ideal for the calculation of EPR data[18]) overestimate delocalization.[19] Moreover, owing to the diminished delocalization, solvent and ion-pairing effects play a decisive role for the radical anions, thus leading to confined electron delocalization. This subtle interplay of effects will be addressed in a separate publication.

However, our investigation clearly shows that rather remarkably, and in contrast to $9^{\bullet-}$, the charge is localized at the DCV moiety adjacent to the acetylenic triple bond in the radical anions of **4** and **5** (see also the Conclusions).

In the case of the [4]dendralenes **1**–**3**, one-electron reduction leads to very well resolved EPR spectra. Based on the identical electron-accepting chromophore in the center of the molecules, the splitting patterns in the spectra are basically matching (Figure 5).

They are dominated by nine equidistant lines spaced by 0.116 ($1^{\bullet-}$) or 0.118 ($2^{\bullet-}$, $3^{\bullet-}$) mT and matching *g*-factors, in line with a structure containing four (virtually) equivalent nitrogen atoms. Here, the spin distribution and the hyperfine data are very well predicted by the theoretical calculations. The spin and the charge are distributed in the central tetracyanobutadiene moiety of the radical anions $1^{\bullet-}$–$3^{\bullet-}$ (Figure 6).

3. CONCLUSIONS

The first example of an unsymmetrically donor-substituted octacyano[4]dendralene (**1**) is reported. With respect to the electronic properties, doubling of the 1,1,4,4-tetracyanobuta-1,3-diene chromophore on going from **4**, **5**, and related TCBDs[8] to octacyano[4]dendralenes **1**–**3** leads to electron acceptors with substantially enhanced electron-accepting power, mirrored by the markedly shifted reduction potentials toward less negative values in **1**–**3**. Whereas tetracyano derivatives **4** and **5** are reduced at −0.81 and −0.95 V vs Fc^+/Fc, respectively,[12] octacyano[4]dendralenes **1**–**3** take up the additional electron already at values of −0.1 ± 0.02 V vs Fc^+/Fc. This is quite a remarkable shift, which should also be analyzed in view of **8** and **9** (Scheme 1),[8b] closely related to **4** and **5** but carrying exclusively *N*,*N*-dimethylaniline substituents as electron-donating groups. The corresponding reduction potentials are −0.69 and −0.89 V vs Fc^+/Fc in line with the additional anilino substituent in **9** diminishing the electron-accepting power.[8b] In view of the notorious contamination by radical anion impurities as a result of their exceptional electron-accepting power, the octacyano[4]dendralenes could not be characterized by high-resolution NMR spectroscopy, but rather X-ray crystal structures were obtained to unambiguously support the structures of derivatives **1**–**3**.

Comparing **4** and **9** renders unexpected aspects: The $E_{1/2(red)}$ values of these two molecules are rather similar; nevertheless, the topologies of these molecules in the solid state are clearly different. Ferrocene derivative **4** (the same holds for its analog **5**) displays an s-*cis*-type arrangement of the two DCV moieties.[12] In contrast, **9** is an (somehow distorted) s-*trans* isomer. The EPR spectra attributed to $9^{\bullet-}$[8c] and $4^{\bullet-}$($5^{\bullet-}$) reveal rather divergent spin distributions. The EPR pattern very clearly shows the presence of four virtually equivalent nitrogen atoms in the case of $9^{\bullet-}$[8c] whereas the spin is confined to only two N atoms (one DCV unit) in the case of $4^{\bullet-}$. These finding points to two prominent conclusions: (i) The s-*cis* orientation established for parent **4** and **5** by X-ray structure analysis is retained in the corresponding radical anions (and incorrectly predicted by calculations, see above), and (ii) the shifts of reduction potentials observed in the series of the TCBD derivatives are based on electronic *and* topological factors. This subtle interplay of effects could only be established by the combination of electrochemical measurements and EPR spectroscopy. However, in the octacyano[4]dendralenes, such

dx.doi.org/10.1021/jo301194y | J. Org. Chem. 2013, 78, 1760–1767

effects are essentially ruled out by the fact that the central tetracyanobuta-1,3-diene core dominates the first reduction, whereas the "outer" DCV moieties serve as interfaces. These effects will be further elaborated using optical spectroscopy.

4. EXPERIMENTAL SECTION

Compounds **2**,[11] **4**,[12] **5**,[12] **7**,[20] **8**,[8b] and **9**[8b] were synthesized according to literature procedures.

X-ray Analysis of Compounds 1 and 3. The X-ray intensity data were measured with Cu Kα radiation (λ = 1.54178 Å) and a mirror optics monochromator for **1** and with Mo Kα radiation (λ = 0.71073 Å) and a graphite monochromator for **3**. Cell dimensions were obtained based upon the refinement of the XYZ-centroids of reflections above 20 $\sigma(I)$. The structure was solved by direct methods and refined using OLEX2 and SHELXS.[21] All non-hydrogen atoms in **1** were refined anisotropically by full matrix least-squares using experimental weights $w = 1/[s^2(F_o)^2 + (0.1000\ P)^2\ ]$, where $P = (F_o^2 + 2\ F_c^2)/3$. For compound **3**, the low number of observed reflexions did not allow to refine all non-H atoms anisotropically. H-atom positions were calculated and included in the structure factor calculation.

Suitable crystals were obtained by layering of a solution of **1** in CH_2Cl_2 with *n*-hexane and subsequent slow evaporation of the solvents. $C_{34}H_{19}FeN_9$, M_r = 609.43 crystal dimensions 0.01 × 0.04 × 0.08 mm monoclinic, space group $P2_1/c$, Z = 4, a = 7.4036(5) Å, b = 40.272(3) Å, c = 9.8627(6) Å, β = 104.307(5)°, V = 2849.5(3) Å^3, D = 1.421 g cm^{-3}at 100(2) K. Numbers of measured and unique reflections were 12734 and 4125, respectively (R_{int} = 0.146). Final $R(F)$ = 0.0603, $wR(F^2)$ = 0.1540 for 399 parameters and 2705 reflections with $I > 2\sigma(I)$ and 2.19 <θ < 60.23° (corresponding R values based on all 4125 reflections are 0.1535 and 0.1831, respectively). CCDC deposition no. 883490.

Suitable crystals of **3** were obtained by layering of a solution of **3** in CH_2Cl_2 with *n*-hexane and subsequent slow evaporation of the solvents. $C_{52}H_{28}N_{10}{\cdot}2CH_2Cl_2$, M_r = 962.70; crystal dimensions 0.02 × 0.2 × 0.3 mm triclinic, space group $P\bar{1}$, Z = 2, a = 8.480(3) Å, b = 15.471(4) Å, c = 18.112(5) Å, α = 91.016°, β = 94.203(8)°, γ = 93.318(8)°, V = 2365.2(12) Å^3 D = 1.352 g cm^{-3}at 100(2) K. Crystal structure contains disordered CH_2Cl_2 molecules. Numbers of measured and unique reflections were 18025 and 8382, respectively (R_{int} = 0.0882). Final $R(F)$ = 0.0956, $wR(F^2)$ = 0.2149 for 625 parameters and 3665 reflections with $I > 2\sigma(I)$ and 1.13 <θ < 25.77° (corresponding R values based on all 8382 reflections are 0.2141 and 0.2696, respectively). CCDC deposition no. 883491.

EPR Measurements. EPR spectra were recorded at ambient temperature. Spectra simulations were performed by means of WinSim, a public domain program.[22]

Chemical Reductions. Reductions were performed in dry THF or CH_2Cl_2 with the use of Na metal. THF was heated to reflux over a Na/K alloy and stored over a Na/K alloy under high vacuum. Its deep blue color in combination with benzophenone was used as an indicator for rigorously water-free conditions. CH_2Cl_2 was dried by heating to reflux over molecular sieves and stored under high vacuum (min. 10^{-5} mbar). Samples were prepared in a special three-compartment EPR sample tube connected to the vacuum line. A Na metal mirror was sublimated to the wall of the tube, and about 0.4 mL of THF or CH_2Cl_2 were freshly condensed to dissolve the investigated compound. The sample was successively degassed by three freeze–pump–thaw cycles and sealed under high vacuum. Reductions were performed by contact of the THF or CH_2Cl_2 solution of the parent molecule with the Na metal mirror in the evacuated sample tube. The sample tubes were either stored at 190 K (2-propanol/dry ice bath) or immediately transferred into the microwave cavity of the EPR spectrometer.

Chemical Oxidation. The dry degassed CH_2Cl_2 sample solutions were prepared by the procedure described above. Oxidation was performed by the mixing of the parent compound solution with selected oxidant (phenyliodine(III) bistrifluoroacetate (PIFA) or $NOSbF_6$) in the evacuated sealed EPR tube. Unfortunately, none of the samples prepared in this way was able to provide an EPR signal that could be unambiguously assigned to the corresponding radical cation.

Electrochemical Reduction/Oxidation. The radical anions of the investigated compound were also prepared by the controlled potential electrolysis of approximately 1 mM CH_3CN sample solutions, containing 0.1 M *n*-Bu_4NClO_4 as supporting electrolyte. The solutions were purged by Ar for 15 min and transferred to the three electrode EPR electrochemical flat cell (Pt mesh working electrode, Pt wire the auxiliary electrode, and Ag wire the pseudoreference electrode). Electrolysis was performed in situ in the cavity of the EPR spectrometer using the Uniscan PG580 potentiostat to set the electrode potential about 100 mV more negative/positive than the $E_{1/2}$ of the redox process under study. Also in this case, the anodic oxidation failed to produce EPR spectra that could be assigned to the corresponding radical cations.

Quantum Chemical Calculations. Calculations were carried out with the Gaussian 03 package.[23] Geometry optimizations (vibrational frequency of stationary points was checked) and single-point determinations of the Fermi contacts (hfcs), were conducted at the B3LYP[24] level of theory with the basis set 6-31G(d).[25]

[1,1,6,6-Tetracyano-3,4-bis(dicyanomethylene)-5-[4-(dimethylamino)phenyl]-1,5-hexadien-2-yl]ferrocene (1). A solution of **5** (129 mg, 0.27 mmol) and TCNE (69 mg, 0.54 mmol) in 1,1,2,2-tetrachloroethane (25 mL) was heated at 80 °C for 6 d under inert atmosphere. The solvent was evaporated and the residue subjected to FC (SiO_2; CH_2Cl_2; R_f = 0.29) to afford **1** (128 mg, 78%) as a dark brown solid: mp >300 °C; IR (ATR) ν = 3126 (w), 2916 (w), 2848 (w), 2216 (m), 1605 (s), 1573 (w), 1517 (s), 1490 (s), 1467 (s), 1434 (s), 1412 (m), 1390 (s), 1336 (s), 1297 (s), 1245 (w), 1211 (s), 1176 (s), 1144 (m), 1110 (m), 1055 (m), 996 (w), 941 (m), 876 (w), 837 (m), 816 (s), 738 (m), 692 (m), 671 (m), 656 (m), 636 (s), 611 cm^{-1} (m); UV/vis (CH_2Cl_2) λ_{max} (ε) = 355 (10 500), 496 (21 600), 668 nm (3 300 M^{-1} cm^{-1}); HR-MALDI-MS (3-HPA) m/z calcd for $C_{34}H_{19}FeN_9^-$ 609.119, found 609.117 (100, [M]$^-$). X-ray: see Figure 1. Because of consistent contamination with radical anion, also in the absence of reducing agent, resolved NMR spectra could not be obtained.

3,4-Bis(dicyanomethylidene)-2,5-bis[4-(diphenylamino) phenyl]hexa-1,5-diene-1,1,6,6-tetracarbonitrile (3). A solution of **7** (51 mg, 0.095 mmol) and TCNE (98 mg, 0.77 mmol) in 1,1,2,2-tetrachloroethane (5.0 mL) was heated at 95 °C for 5 d under inert atmosphere. The solvent was evaporated and the residue subjected to FC (SiO_2; CH_2Cl_2) to afford **3** (12 mg, 18%) as a black solid: mp >300 °C; IR (ATR) ν = 3062 (w), 2617 (w), 2220 (m), 1607 (s), 1583 (w), 1522 (s), 1480 (s), 1441 (s), 1323 (s), 1287 (s), 1179 (s), 1074 (m), 1001 (w), 900 (m), 824 (w), 754 (m), 719 (m), 693 (m), 634 (m), 618 cm^{-1} (m); λ_{max} (ε) = 278 (25 600), 474 (25 800), 521 nm (26 300 M^{-1} cm^{-1}); HR-MALDI-MS (3-HPA) m/z calcd for $C_{52}H_{28}N_{10}^-$ 792.2504, found 792.2516 (100, [M]$^-$). X-ray: see Figure 1. Because of consistent contamination with radical anion, also in the absence of reducing agent, resolved NMR spectra could not be obtained.

■ ASSOCIATED CONTENT

Supporting Information

Calculated geometries and hfcs of $\mathbf{1}^{\bullet-}$ to $\mathbf{4}^{\bullet-}$. X-ray crystallography details and CIF files. This material is available free of charge via the Internet at http://pubs.acs.org/

■ AUTHOR INFORMATION

Corresponding Author

*E-mail: diederich@org.chem.ethz.ch, g.gescheidt-demner@tugraz.at.

Notes

The authors declare no competing financial interest.

In Memoriam Howard E. Zimmerman

■ ACKNOWLEDGMENTS

This work was supported by the ERC Advanced Grant No. 246637 (OPTELOMAC) and by the FWF (Austria, project no. P20019-N17). B.B. is grateful for a Kekulé fellowship from the Fonds der Chemischen Industrie (VCI). D.T. was the recipient of a JSPS postdoctoral fellowship.

■ REFERENCES

(1) Gompper, R.; Wagner, H. U. *Angew. Chem., Int. Ed.* **1988**, *27*, 1437−1455.

(2) (a) Faupel, F.; Dimitrakopoulos, C.; Kahn, A.; Woll, C. *J. Mater. Res.* **2004**, *19*, 1887−1888. (b) Roncali, J.; Leriche, P.; Cravino, A. *Adv. Mater.* **2007**, *19*, 2045−2060. (c) Barlow, S.; Marder, S. R. In *Functional Organic Materials*; Müller, T. J. J., Bunz, U. H. F., Eds.; Wiley-VCH: Weinheim, 2007; pp 393−437. (d) Forrest, S. R.; Thompson, M. E. *Chem. Rev.* **2007**, *107*, 923−925. (e) Kivala, M.; Diederich, F. *Acc. Chem. Res.* **2009**, *42*, 235−248. (f) Kato, S.-I.; Diederich, F. *Chem. Commun.* **2010**, 1994−2006. (g) Miller, R. D.; Chandross, E. A. *Chem. Rev.* **2010**, *110*, 1−574.

(3) (a) Tykwinski, R. R.; Schreiber, M.; Gramlich, V.; Seiler, P.; Diederich, F. *Adv. Mater.* **1996**, *8*, 226−231. (b) Blanchard-Desce, M.; Alain, V.; Bedworth, P. V.; Marder, S. R.; Fort, A.; Runser, C.; Barzoukas, M.; Lebus, S.; Wortmann, R. *Chem.—Eur. J.* **1997**, *3*, 1091−1104. (c) Tykwinski, R. R.; Gubler, U.; Martin, R. E.; Diederich, F.; Bosshard, C.; Gunter, P. *J. Phys. Chem. B* **1998**, *102*, 4451−4465. (d) Dalton, L. R. *J. Phys.: Condens. Matter* **2003**, *15*, R897−R934. (e) May, J. C.; Biaggio, I.; Bureš, F.; Diederich, F. *Appl. Phys. Lett.* **2007**, *90*, 2511061−2511063. (f) Frank, B.; La Porta, P.; Breiten, B.; Kuzyk, M. C.; Jarowski, P. D.; Schweizer, W. B.; Seiler, P.; Biaggio, I.; Boudon, C.; Gisselbrecht, J.-P.; Diederich, F. *Eur. J. Org. Chem.* **2011**, 4307−4317.

(4) (a) Cairns, T. L.; Carboni, R. A.; Coffman, D. D.; Engelhardt, V. A.; Heckert, R. E.; Little, E. L.; McGeer, E. G.; McKusick, B. C.; Middleton, W. J. *J. Am. Chem. Soc.* **1957**, *79*, 2340−2341. (b) Webster, O. W. *J. Polym. Sci., Part A: Polym. Chem.* **2002**, *40*, 210−221.

(5) (a) Fatiadi, A. J. *Synthesis* **1986**, 249. (b) Fatiadi, A. J. *Synthesis* **1987**, 959. (c) Fatiadi, A. J. *Synthesis* **1987**, 749−789. (d) Miller, J. S. *Angew. Chem., Int. Ed.* **2006**, *45*, 2508−2525.

(6) (a) Acker, D. S.; Harder, R. J.; Hertler, W. R.; Mahler, W.; Melby, L. R.; Benson, R. E.; Mochel, W. E. *J. Am. Chem. Soc.* **1960**, *82*, 6408−6409. (b) Acker, D. S.; Hertler, W. R. *J. Am. Chem. Soc.* **1962**, *84*, 3370−3374.

(7) (a) Wheland, R. C.; Martin, E. L. *J. Org. Chem.* **1975**, *40*, 3101−3109. (b) Martin, N.; Segura, J. L.; Seoane, C. *J. Mater. Chem.* **1997**, *7*, 1661−1676. (c) Hünig, S.; Herberth, E. *Chem. Rev.* **2004**, *104*, 5535−5563. (d) Segura, J. L.; Gómez, R.; Seoane, C. *Chem. Soc. Rev.* **2007**, *36*, 1305−1322.

(8) (a) Michinobu, T.; May, J. C.; Lim, J. H.; Boudon, C.; Gisselbrecht, J.-P.; Seiler, P.; Gross, M.; Biaggio, I.; Diederich, F. *Chem. Commun.* **2005**, 737−739. (b) Michinobu, T.; Boudon, C.; Gisselbrecht, J.-P.; Seiler, P.; Frank, B.; Moonen, N. N. P.; Gross, M.; Diederich, F. *Chem.—Eur. J.* **2006**, *12*, 1889−1905. (c) Kivala, M.; Stanoeva, T.; Michinobu, T.; Frank, B.; Gescheidt, G.; Diederich, F. *Chem.—Eur. J.* **2008**, *14*, 7638−7647. (d) Kivala, M.; Boudon, C.; Gisselbrecht, J.-P.; Enko, B.; Seiler, P.; Muller, I. B.; Langer, N.; Jarowski, P. D.; Gescheidt, G.; Diederich, F. *Chem.—Eur. J.* **2009**, *15*, 4111−4123.

(9) This transformation had originally been reported for metal (Pt, Ru) acetylides: (a) Bruce, M. I.; Rogers, J. R.; Snow, M. R.; Swincer, A. G. *J. Chem. Soc., Chem Commun.* **1981**, 271−272. (b) Bruce, M. I. *Aust. J. Chem.* **2011**, *64*, 77−103.

(10) For recent examples, see: (a) Morimoto, M.; Murata, K.; Michinobu, T. *Chem. Commun.* **2011**, *47*, 9819−9821. (b) Chiu, M.; Jaun, B.; Beels, M. T. R.; Biaggio, I.; Gisselbrecht, J.-P.; Boudon, C.; Schweizer, W. B.; Kivala, M.; Diederich, F. *Org. Lett.* **2012**, *14*, 54−57.

(11) Breiten, B.; Wu, Y. L.; Jarowski, P. D.; Gisselbrecht, J. P.; Boudon, C.; Griesser, M.; Onitsch, C.; Gescheidt, G.; Schweizer, W. B.; Langer, N.; Lennartz, C.; Diederich, F. *Chem. Sci.* **2011**, *2*, 88−93.

(12) Jordan, M.; Kivala, M.; Boudon, C.; Gisselbrecht, J.-P.; Schweizer, W. B.; Seiler, P.; Diederich, F. *Chem. Asian J.* **2011**, *6*, 396−401.

(13) (a) Brown, H. C.; Okamoto, Y. *J. Am. Chem. Soc.* **1958**, *80*, 4979−4987. (b) Hansch, C.; Leo, A.; Taft, R. W. *Chem. Rev.* **1991**, *91*, 165−195.

(14) Jayamurugan, G.; Gisselbrecht, J.-P.; Boudon, C.; Schoenebeck, F.; Schweizer, W. B.; Bernet, B.; Diederich, F. *Chem. Commun.* **2011**, *47*, 4520−4522.

(15) Moonen, N. N. P.; Pomerantz, W. C.; Gist, R.; Boudon, C.; Gisselbrecht, J.-P.; Kawai, T.; Kishioka, A.; Gross, M.; Irie, M.; Diederich, F. *Chem.—Eur. J.* **2005**, *11*, 3325−3341.

(16) (a) Gescheidt, G. In *Electron Paramagnetic Resonance: A Practitioner's Toolkit*; Brustolon, M., Giamello, E., Eds.; Wiley & Sons: Hoboken, NJ, 2009; pp 109−157. (b) Davies, A. G. *J. Chem. Res., Synop.* **2001**, 253−261.

(17) (a) Prins, R. *Mol. Phys.* **1970**, *19*, 603−620. (b) Duggan, D. M.; Hendrickson, D. N. *Inorg. Chem.* **1975**, *14*, 955−970. (c) Ammeter, J. H. *J. Magn. Reson.* **1978**, *30*, 299−325. (d) Prins, R.; Korswagen, A. R. *J. Organomet. Chem.* **1970**, *25*, C74−C76.

(18) (a) Hermosilla, L.; Calle, P.; de la Vega, J. M. G.; Sieiro, C. *J. Phys. Chem. A* **2006**, *110*, 13600−13608. (b) Hermosilla, L.; Garcia de la Vega, J. M.; Sieiro, C.; Calle, P. *J. Chem. Theor. Comput.* **2011**, *7*, 169−179. (c) Puzzarini, C.; Barone, V. *J. Chem. Phys.* **2010**, *133*, 184301−184311. (d) Batra, R.; Giese, B.; Spichty, M.; Gescheidt, G.; Houk, K. N. *J. Phys. Chem.* **1996**, *100*, 18371−18379.

(19) Bally, T.; Sastry, G. N. *J. Phys. Chem. A* **1997**, *101*, 7923−7925.

(20) Lambert, C.; Nöll, G. *Synth. Met.* **2003**, *139*, 57−62.

(21) (a) Dolomanov, O. V.; Bourhis, L. J.; Gildea, R. J.; Howard, J. A. K.; Puschmann, H. *J. Appl. Crystallogr.* **2009**, *42*, 339−341. (b) Sheldrick, G. M. *Acta Crystallogr. A* **2008**, *64*, 112−122.

(22) Duling, D. R. *J. Magn. Reson. B* **1994**, *104*, 105−110.

(23) Frisch, M. J.; Trucks, G. W.; Schlegel, H. B.; Scuseria, G. E.; Robb, M. A.; Cheeseman, J. R.; Montgomery, J. A., Jr.; Vreven, T.; Kudin, K. N.; Burant, J. C.; Millam, J. M.; Iyengar, S. S.; Tomasi, J.; Barone, V.; Mennucci, B.; Cossi, M.; Scalmani, G.; Rega, N.; Petersson, G. A.; Nakatsuji, H.; Hada, M.; Ehara, M.; Toyota, K.; Fukuda, R.; Hasegawa, J.; Ishida, M.; Nakajima, T.; Honda, Y.; Kitao, O.; Nakai, H.; Klene, M.; Li, X.; Knox, J. E.; Hratchian, H. P.; Cross, J. B.; Bakken, V.; Adamo, C.; Jaramillo, J.; Gomperts, R.; Stratmann, R. E.; Yazyev, O.; Austin, A. J.; Cammi, R.; Pomelli, C.; Ochterski, J. W.; Ayala, P. Y.; Morokuma, K.; Voth, G. A.; Salvador, P.; Dannenberg, J. J.; Zakrzewski, V. G.; Dapprich, S.; Daniels, A. D.; Strain, M. C.; Farkas, O.; Malick, D. K.; Rabuck, A. D.; Raghavachari, K.; Foresman, J. B.; Ortiz, J. V.; Cui, Q.; Baboul, A. G.; Clifford, S.; Cioslowski, J.; Stefanov, B. B.; Liu, G.; Liashenko, A.; Piskorz, P.; Komaromi, I.; Martin, R. L.; Fox, D. J.; Keith, T.; Al-Laham, M. A.; Peng, C. Y.; Nanayakkara, A.; Challacombe, M.; Gill, P. M. W.; Johnson, B.; Chen, W.; Wong, M. W.; Gonzalez, C.; Pople, J. A. Gaussian 03, Revision E.01; Gaussian, Inc.: Wallingford, CT, 2004.

(24) (a) Becke, A. D. *J. Chem. Phys.* **1993**, *98*, 5648−5652. (b) Stephens, P. J.; Devlin, F. J.; Chabalowski, C. F.; Frisch, M. J. *J. Phys. Chem.* **1994**, *98*, 11623−11627.

(25) Hariharan, P. C.; Pople, J. A. *Theor. Chim. Acta* **1973**, *28*, 213−222.